3

Computational Industrial Mechanics Programme (CIMP)

Sophisticated mathematical modelling aided by powerful computing and visualization has the potential to provide the cutting-edge to industry; generation of cost-effective solutions, process optimization and product design are some of the areas where modelling and simulation can play critical to enabling role. The C-MMACS Computational Industrial Mechanics Programme (CIMP) seeks to develop and apply tools of mathematical modelling and computer simulation in diverse areas of engineering.

Highlights

The Year 2004-05 for CIMP is characterized by development and refinement of a number of theoretical and conceptual issues in the areas of finite element analysis, elastodynamics, numerical algorithms and non-linear dynamics.

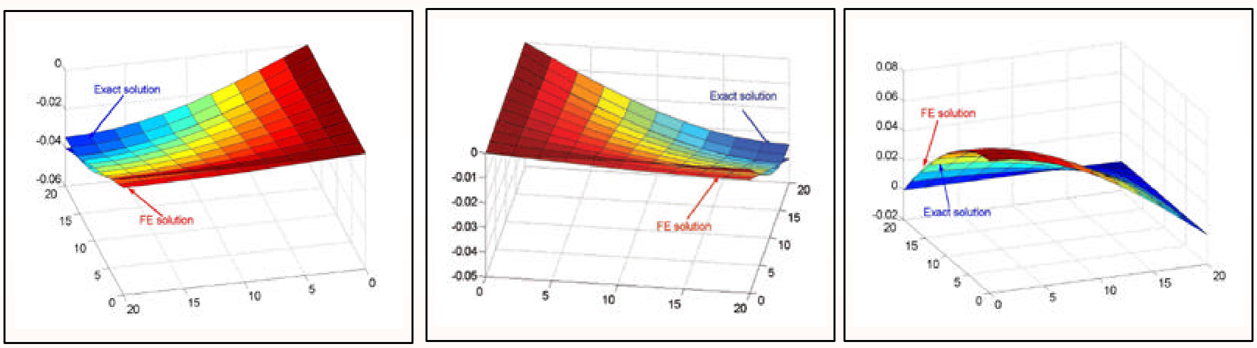

Analysis results with a quarter plate model of a simply supported plate subjected sinusoidal load: The analytical solution and the finite element solution using the BFS model (a) variation of d^2w/dx^2. (b)variation of d^2w/dy^2 . (c) variation of $2*d^2w/(dxdy)$.

Inside

- *Mesh Distortion Immunity of Finite Elements and the Best-Fit Paradigm*
- *A Function Space Approach to study Rank Deficiency and Spurious Modes in Finite Elements.*
- *Analysis of ACM and BFS Elements using the Function Space Approach*
  - *Elastostatic Problems*
  - *Elastodynamic Problems*
- *Development of New Runge-Kutta Nystrom Methods*
- *Dynamics and Rheology of Periodically Forced Suspensions*

3.1 Mesh Distortion Immunity of Finite Elements and the Best-Fit Paradigm

Distortion of finite element meshes often lead to poor results. One solution is to use unsymmetric formulation to restore the mesh distortion immunity. There are two separate sets of shape functions that are used in such formulations. The first set of shape functions (parametric shape functions) should satisfy the minimum inter- as well as intra-element displacement continuity requirements and the second set of shape functions(metric shape functions) should satisfy all the linear and higher order completeness requirements and has to produce quadratic displacement field. Depending on the shape function used, the elements are classified into parametric (PP), metric (MM), parametric-metric (PM) and metric-parametric elements (MP). Numerical tests are carried out for a single element three-noded bar element of length L with nodes at x_1, x_2 and x_3 with uniform traction load. We assume that the node x_2 is not at the centre of the bar so that the distortion parameter $\Delta = x_2 - L/2$. The numerical test results prove that the PP and PM elements give the exact displacements when there is no distortion ($\Delta = 0$) as shown in Table 3.1. When there is distortion, only the PM formulation is insensitive to distortion. The behaviour of the PP and PM elements are explained using the best-fit paradigm.

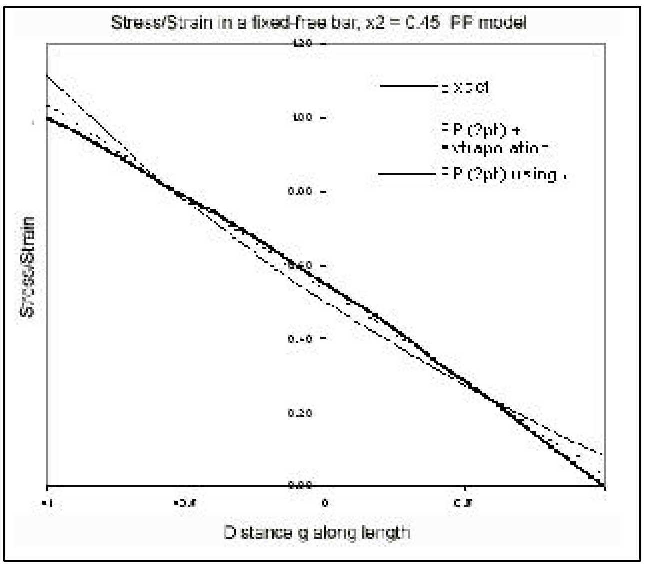

Fig 3.1 The variation of stress in a fixed-free bar for uniformly distributed load x_2=0.45 for Parametric Model

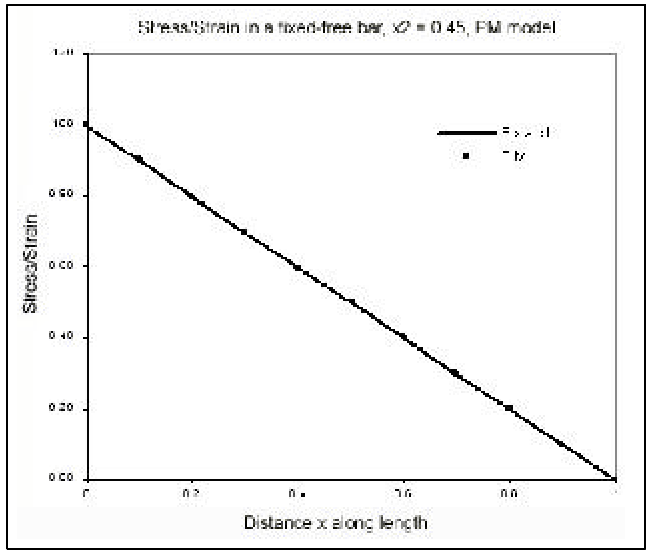

Fig 3.2 The variation of stress in a fixed-free bar for uniformly distributed load when x_2 =0.45 for Parametric-Metric Model

Fig 3.1 shows that the strain/stress is computed using the parametric transformation involving the Jacobian *J* in the denominator; the variation of strain thus computed is as shown by the thin solid line. The dashed line indicates the extrapolation of stress from the Gauss point values used for the 2-pt Gaussian numerical integration of the PP stiffness matrix. This is a closer approximation of the actual variation of strain and explains why the 2-pt. rule is favoured in most industry standard packages. Fig 3.2 shows the stress/strain recovered from the displacements computed using the PM element for the case with distortion. The PM formulation is insensitive to mesh distortion because the strain is in metric space (shown by the thick solid line).

Table 3.1 Deflections u_2 and u_3 for a single-element test of fixed-free bar with uniform traction load of q = 1

Displacements	$\Delta = 0$			$\Delta = -0.05$		
	PP	PM	Exact	PP	PM	Exact
u_2	0.37500	0.37500	0.37500	0.34833	0.34875	0.34875
u_3	0.50000	0.50000	0.50000	0.50000	0.50000	0.50000

3.2 A Function Space Approach to Study Rank Deficiency and Spurious Modes in Finite Elements.

Finite elements based on isoparametric formulation are known to suffer spurious stiffness properties and corresponding stress oscillations, even when care is taken to ensure that completeness and continuity requirements are enforced. This occurs frequently when the physics of the problem requires multiple strain components to be defined. This kind of error, commonly known as locking, can be circumvented by using reduced integration techniques to evaluate the element stiffness matrices instead of the full integration that is mathematically prescribed. However, the reduced integration technique itself can have a further drawback - rank deficiency, which physically implies that spurious energy modes (e.g., hourglass modes) are introduced because of reduced integration. Such instability in an existing stiffness matrix is generally detected by means of an eigenvalue test. In this work we have shown that a knowledge of the dimension of the solution space B spanned by the column vectors of the strain-displacement matrix can be used to identify the instabilities arising in an element due to reduced/ selective integration techniques a priori, without having to complete the element stiffness matrix formulation and then test for zero eigenvalues. The rank deficiency of two noded and three noded Timoshenko beam elements, quad4 element and Mindlin plate element have been examined for various quadrature schemes. The results for the QUAD4 element have been shown in Table 3.2. This element has 4 nodes with 2 dof at each node, so that number of degrees of freedom per element N_f =8. The number of rigid body modes physically permissible is three i.e. $N_r^p = 3$. Therefore the proper rank of the stiffness matrix K_e=5. When a 2x2 Gauss quadrature is used to evaluate the stiffness matrix the dimension of B space is 5, which is equal to the proper rank of K_e. In case of one point Gauss quadrature the rank of K_e=3 indicating that the element has a rank deficiency 2. The dimension of *B** space is now 3 which is obtained by finding the basis vectors of the [*B**] matrix. The [*B**] matrix is obtained from the [*B*] matrix by dropping the higher order polynomial terms. This suggests that the dimension of the solution space is a good measure to detect rank deficiency in an element stiffness matrix and can be used for deciding an optimal integration strategy to eliminate locking. Integrating this test with a finite element program, use of an element that contains a possible instability can be avoided and the accuracy of finite element analysis can be increased.

Table 3.2 The results for the QUAD4 element

$$\left(N_f = 8, N_r^p = 3\right) Rank\ Deficiency = 2\ \dim B \neq \dim B^*$$

Element type	Integration rule	Rank of K_e (no. of nonzero)	No. of Mechanisms	Dimensions B or B*
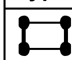	Full	5	0	5
Four noded (8 d.o.f)	Reduced	3	2	3

K Sangeeta, S Mukherjee and G Prathap

3.3 Analysis of ACM and BFS Elements using the Function Space Approach

3.3.1 Elastostatic Problems

The finite element formulations of Kirchhoff plate bending model are quite complex. The complexity arises due to the nature of the higher order partial differential equation needed to describe the problem. There are many formulations available in the literature for Kirchhoff plate bending finite element model. The most popular rectangular Kirchhoff plate bending finite element models are the ACM and BFS elements. The former element has three degrees of freedom per node and the latter has four degrees of freedom per node.

The Kirchhoff finite element plate bending model requires C^1 continuity, i.e., the transverse displacement w and the normal slope $w_{,n}$ should be continuous across the inter element boundary.

The BFS element meets all the continuity requirements. However, the ACM element does not ensure the continuity of the normal slope across the inter element boundaries.

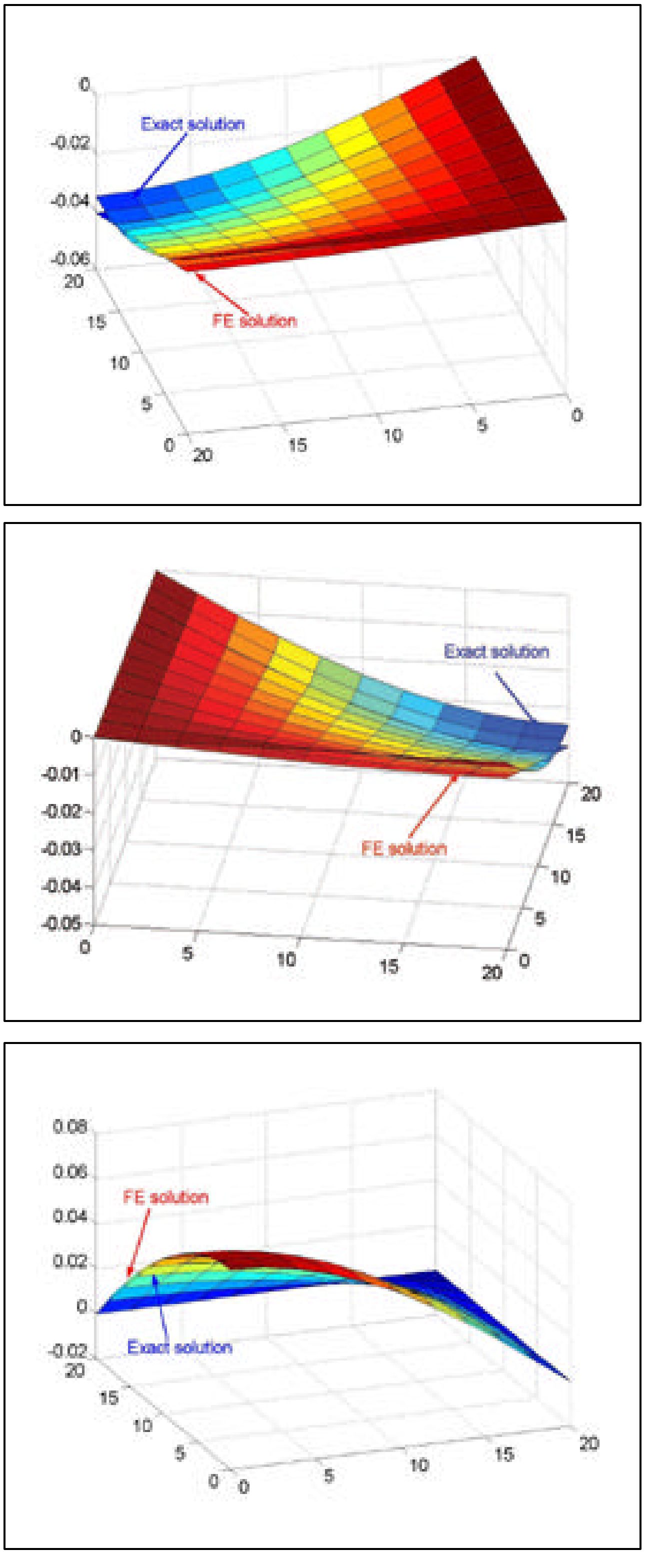

Fig 3.3 Analysis results with a quarter plate model of a simply supported plate subjected sinusoidal load: The analytical solution and the finite element solution using the BFS model (a) variation of d^2w/dx^2 (b) variation of d^2w/dy^2(c) variation of $2*d^2w/(dxdy)$.

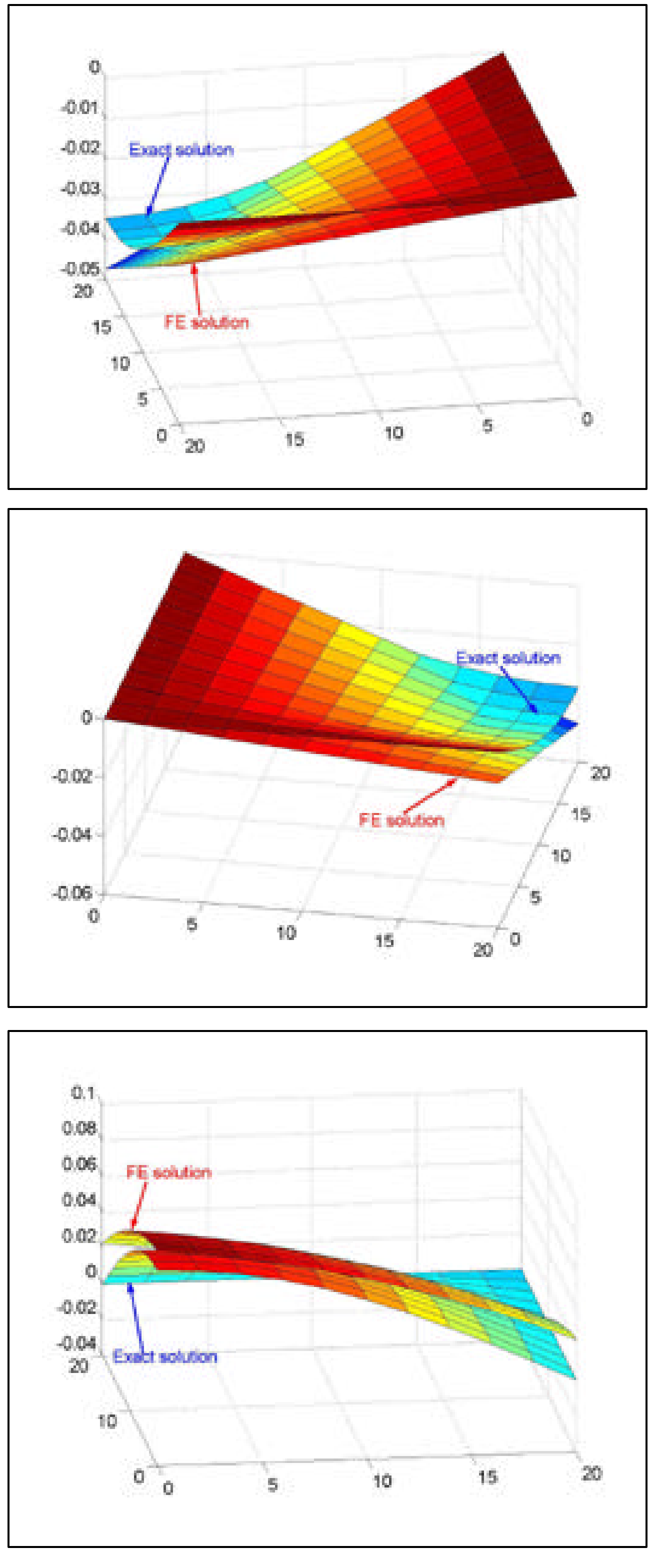

Fig 3.4 Analysis results with a quarter plate model of a simply supported plate subjected sinusoidal load: The analytical solution and the finite element solution using the ACM model (a) variation of d^2w/dx^2 (b) variation of d^2w/dy^2(c) variation of $2*d^2w/(dxdy)$.

Numerical experiment data

Length of the plate L_x=40; L_y=40; Thickness t=0.4; Poisson's ratio n=0.3; Young's modulus of elasticity E=2x10^5; Mass density r =7850x10^{-9}

Table 3.3 The result of the numerical experiment

	$\langle e,e \rangle$ (1)	$\langle \bar{e},\bar{e} \rangle$ (2)	$\langle \bar{e},e \rangle$ (3)	$\|e-\bar{e}\|^2$ (4)	$\|e\|^2-\|\bar{e}\|^2$ (5)	$\langle \bar{e},e-\bar{e} \rangle$ (6)
BSF	560.5226	558.0822	558.0822	2.4404	2.4404	0
ACM	560.5226	671.9582	602.5109	27.459	-111.4355	69.4473

In the present work, we re-examine both the ACM and BFS formulations from the variational calculus point of view. It is observed that the BFS element satisfies the virtual work principle at the element level and hence, the finite element strain obtained from the BFS model is the best-fit strain ε at the element level and also at the global level. It also satisfies the energy error rule. However, the ACM element violates the virtual work principle and the finite element strain deviates from the best-fit solution. The present study reveals that the conforming requirement is another necessary condition for the correct variational formulation of the finite element model. It is worth noting here that, *a priori* prediction of the finite element solution is not possible for a variationally incorrect formulation.

A numerical experiment has been presented for the simply supported plate with a sinusoidal load, discretised with 4 elements of ACM and BFS finite element model. The results are presented in Table 3.3. It is shown here that each component of the finite element strain vector obtained from the BFS model are individually the best fit to the corresponding analytical element strain vector component. It is also shown that the BFS model satisfy the virtual work principle. However, the ACM model violates the virtual work principle and hence the best fit rule.

3.3.2 Elastodynamic Problems

In this study, we critically examine the variational correctness of the Kirchhoff finite element elastodynamic plate bending models. The ACM mocel satisfies the elastodynamic energy error rule. However, the ACM finite element elastodynamic model does not satisfy the frequency-error-hyperboloid equation. It is also observed in the "sweep test" that the natural frequencies obtained using ACM model does not offer the upper boundedness with exact solution. This is attributed to the violation of the virtual work principle by the ACM finite element model. The BFS model satisfy the hyperboloid equation and also, the frequencies obtained using the BFS model, are always above the exact solution. The numerical results are presented for the fundamental mode of the simply supported plate in Table 3.4.

Table 3.4 Numerical results for the fundamental mode of the simply supported plate

	$\langle e,e \rangle = w^2(u,u)$	$\langle \bar{e},e \rangle = w^2(\bar{u},u)$	$\langle \bar{e},\bar{e} \rangle = w^2(\bar{u},\bar{u})$
BFS	71.3620	71.3620	234.0468
ACM	71.362	-	2813.1868

P Jafarali, R Muralikrishna, S Mukherjee and G Prathap

3.4 Development of New Runge-Kutta Nystrom Methods

The solution of the initial value problems of second order ordinary differential equations can often be performed with fewer function evaluations by Runge-Kutta Nystrom methods as compared to Runge-Kutta methods. The Runge Kutta Nystrom method for a second order ordinary differential equation can be written as:

$$f_j = f\left(x_i + c_j h, y_i + c_j h y'_i + h^2 \sum_{k=1}^{s} \bar{a}_{jk} f_k , y'_i + h \sum_{k=1}^{s} a_{jk} \right)$$

$$y_{i+1} = y_i + h y'_i + h^2 \sum_{j=1}^{s} b_j f_j$$

$$y'_{i+1} = y'_i + h^2 \sum_{j=1}^{s} b'_j f_j$$

The coefficients in the above equation are determined to a given order by matching the Taylor expansion of the exact solution and the numerical solution. This yields a set of nonlinear algebraic equations. Usually as we increase the number of stages, the number of coefficients in the algorithm increases faster than the number of equations the coefficients have to satisfy (the order conditions). A new Runge-Kutta Nystrom method is obtained by choosing the free parameters so that an optimal method in some sense is obtained. We have noticed that the order conditions are nonlinear and hence multiple solutions of the equations may be obtained. One way of exciting the multiple solutions is by varying the choice of the free parameter. We have demonstrated that the choice of the free parameters influences to a great extent the method obtained. We have shown that depending on the choice of the free parameter, the optimal method in a given sense can be changed significantly.

T R Ramamohan, F O Otunta and S Imoni

3.5 Dynamics and Rheology of Periodically Forced Suspensions

We have continued our work on the rheology of periodically forced suspensions. We have formulated the problem of periodically forced particles in time dependent uniform flow fields including inertial effects. We are in the process of developing software to model the motion of a spherical particle under the action of an external periodic force in a time dependent uniform flow field including inertial effects. We have also prepared a detailed review of our work in this area.

T R Ramamohan